JOURNAL OF BACTERIOLOGY, Sept. 1990, p. 4877–4887
0021-9193/90/094877-11$02.00/0

Vol. 172, No. 9

Developmental Sensory Transduction in *Myxococcus xanthus* Involves Methylation and Demethylation of FrzCD

WILLIAM R. McCLEARY, MARK J. McBRIDE, AND DAVID R. ZUSMAN*

Department of Molecular and Cell Biology, University of California, Berkeley, California 94720

Received 5 March 1990/Accepted 14 June 1990

***Myxococcus xanthus* is a bacterium that moves by gliding motility and exhibits multicellular development (fruiting body formation). The frizzy (*frz*) mutants aggregate aberrantly and therefore fail to form fruiting bodies. Individual *frz* cells cannot control the frequency at which they reverse direction while gliding. Previously, FrzCD was shown to exhibit significant sequence similarity to the enteric methyl-accepting chemotaxis proteins. In this report, we show that FrzCD is modified by methylation and that *frzF* encodes the methyltransferase. We also identify a new gene, *frzG*, whose predicted product is homologous to that of the *cheB* (methylesterase) gene from *Escherichia coli*. Thus, although *M. xanthus* is unflagellated, it appears to have a sensory transduction system which is similar in many of its components to those found in flagellated bacteria.**

Myxococcus xanthus is a gram-negative, rod-shaped soil bacterium whose life cycle is characterized by extensive cell-cell interactions (42, 63). The myxobacteria are essentially primitive multicellular organisms composed of procaryotic cells. Large numbers of cells glide on solid surfaces in feeding swarms, which release hydrolytic enzymes to cooperatively digest nutrients. The mechanisms involved in gliding motility remain unknown, although several hypotheses have been suggested (20, 25, 39). When nutrients become limiting, cells aggregate to a focal center, where they form a mound of approximately 100,000 cells called a fruiting body. In these mounds, the rod-shaped cells differentiate into spherical, metabolically dormant, environmentally resistant myxospores. The concerted nature of their social behavior suggests that intercellular signaling is important in coordinating the many activities of the *M. xanthus* life cycle. Four groups of synergizable sporulation mutants have been isolated (*asg*, *bsg*, *csg*, and *dsg*) which behave as if they are unable to either produce or release extracellular signals (11, 24). These mutants develop when they are in proximity to wild-type cells or cells of the different synergizable groups.

In our attempt to understand the processes involved in development, we isolated a large number of nonfruiting mutants (31). One such class unable to aggregate properly is called frizzy (62). These mutants are unable to form fruiting bodies but instead aggregate to form myxospore-containing frizzy filaments at high cell density and donut-shaped swirls at low cell density. The *frz* genes were cloned and were found to be clustered on the chromosome (Fig. 1) (4). Genetic analysis revealed five complementation groups (*frzA*, *-B*, *-C*, *-E*, and *-F*). Strains with mutations in any one of these genes have the Frz phenotype. Another complementation group, *frzD*, is defined by two Tn*5* mutations mapping in the C terminus of *frzCD*. These mutants form nonspreading colonies of motile cells. Tn*5* insertions in the 1-kilobase-pair (kbp) region between *frzE* and *frzF* define the gap region. These mutants are fruiting proficient, but because of data to be presented in this report, this complementation group is now designated *frzG*. Time lapse video microscopy showed that the *frz* genes are involved in determining the frequency at which cells reverse their direction of gliding (5). Individual *frz* cells reverse their gliding direction less frequently than do wild-type cells, whereas *frzD* cells reverse more frequently. These behavior patterns are reminiscent of chemotaxis mutants of enteric bacteria which swim smoothly and rarely tumble or tumble and rarely swim smoothly.

Escherichia coli is able to sense many components in its environment and to respond by altering its swimming behavior (for reviews, see references 21, 28, and 52). When the peritrichously arranged flagella of *E. coli* rotate counterclockwise, a bundle of rotating flagella is formed and the organism swims smoothly, i.e., runs; clockwise rotation destabilizes the tuft of flagella and causes the cell to tumble. In the absence of a gradient, *E. coli* swims randomly, alternating between runs and tumbles. By controlling the frequency of runs and tumbles, the bacterium swims toward higher nutrient concentrations and away from repellants.

The components of the enteric chemotactic signal transduction pathway include CheA, CheB, CheR, CheY, CheZ, and the methyl-accepting chemotaxis proteins (MCPs). The MCPs are transmembrane receptors that bind chemoeffectors in the periplasm and most likely transduce that information to their cytoplasmic domains through intramolecular conformational changes. The MCPs interact with CheW to transmit their ligand occupancy information to CheA (26, 46), which is the central processing component of this pathway. Upon stimulation, it is autophosphorylated (17); the phosphate group is then rapidly shuttled to either CheY or CheB (16, 66). It is thought that CheY-phosphate interacts with the switch of the flagellar motor and generates a tumble (38, 53). CheZ is a CheY-specific phosphatase which functions as an antagonist of activated CheY (16). The MCPs are regulated by covalent modification to effect desensitization, i.e., adaptation, to new concentrations of chemoeffectors. Specific glutamyl residues of the MCPs are methylated and demethylated by CheR and CheB, respectively (50, 55). The CheA-catalyzed phosphorylation of CheB results in a significant increase in its methylesterase activity (27).

Recently, the nucleotide sequences of several of the *frz* genes were determined (29). Sequence analysis revealed that FrzA and FrzCD were homologous to enteric CheW and to

* Corresponding author.

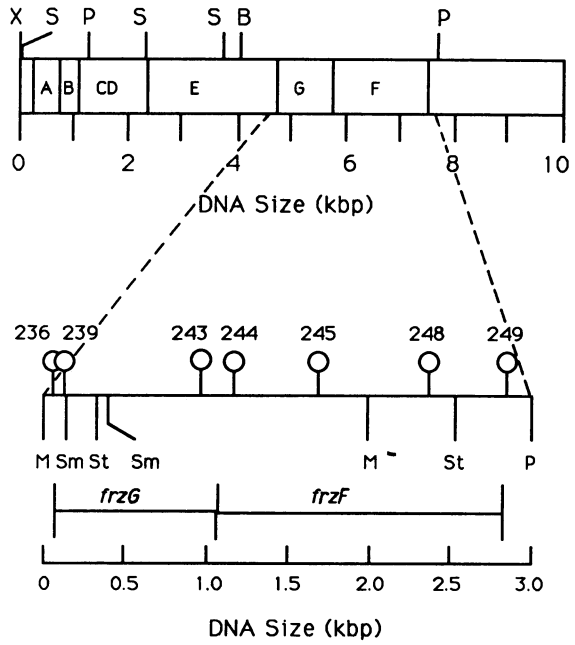

FIG. 1. Physical and genetic map of the *frz* region. The enlarged segment corresponds to the nucleotide sequence presented in Fig. 4 and shows the sites of Tn*5* insertion in *frzG* and *frzF*. ♀ marks Tn*5* insertion sites. Restriction sites: X, *Xho*I; S, *Sst*I; P, *Pts*I; B, *Bgl*II; Sm, *Sma*I; St, *Stu*I; M, *Mlu*I.

the MCPs, respectively. The region of similarity between FrzCD and the enteric MCPs spans the signaling and adaptation domains and includes several of the sites of methylesterification.

In this report, we present further evidence that the frizzy genes constitute a sensory transduction pathway which controls the frequency at which *M. xanthus* cells reverse their direction of gliding and that this sensory transduction utilizes protein methylation and demethylation to modulate the response.

MATERIALS AND METHODS

Strains and culture conditions. The *M. xanthus* strains used in this study are described in Table 1. *M. xanthus* DZF1 (FB) (9) was the parental fruiting-competent strain. Strains containing Tn*5* insertions were constructed as previously described (33). Briefly, generalized transduction with bacteriophage P1 was used to introduce plasmids maintained in *E. coli* into *M. xanthus*. The strains were verified by Southern blot analysis.

TABLE 1. *M. xanthus* strains used

Strain	Genotype	Tn*5* insert[a]	Phenotype	Source or reference
DZF1	*frz*$^+$		Fru$^+$	31
DZF3401	*frzC*	Ω217	Frz Kan^r	4
DZF3460	*frzD*	Ω224	Fru$^-$ Kan^r Nonspreading	This study
DZF4021	*frzG*	Ω239	Fru$^+$ Kan^r	This study
DZF3593	*frzF*	Tn*5-lac*Ω540	Frz Kan^r	60
DZF4023	*frzF*	Ω245	Frz Kan^r	This study
DZF3558	Δ(*frzA-E*)	Ω233	Frz Kan^r	4

[a] These Tn*5* insertions correspond to those previously described by Blackhart and Zusman (4) and Weinberg and Zusman (60).

Vegetative cultures were grown in Casitone-yeast extract (7) broth at 32°C on a rotary shaker at 225 rpm. Development was initiated by concentrating vegetatively grown cells to 1.3 × 10^{10} cells per ml in 10 mM *N*-2-hydroxyethyl-*N'*-2-ethanesulfonic acid (HEPES)–8 mM $MgSO_4$ (HM), after which 0.5 ml was evenly spread onto 150-mm-diameter clone fruiting (CF) (11) medium containing 1.5% agar.

Protein A-FrzCD fusion protein. The protein A-FrzCD fusion was constructed by digesting pBB12 (4) with *Pst*I and *Pvu*II and ligating the 1.2-kilobase fragment into *Pst*I-*Eco*RV-cut pRIT2T (Pharmacia LKB Biotechnology, Piscataway, N.J.). The resulting plasmid containing an open reading frame encoding 268 residues of protein A followed by 367 residues of FrzCD was cloned and maintained in *E. coli* N4830-1. Cells were grown in LB broth containing 100 μg of ampicillin per ml at 30°C to a density of 100 to 200 Klett units. An equal volume of 54°C LB was added, and incubation was continued for 2 h at 42°C to allow expression of the fusion protein from the λ p_R promoter. Cells were harvested by centrifugation and stored at −70°C. Cells were disrupted in 50 mM Tris hydrochloride (pH 7.0)–150 mM NaCl–5 mM EDTA–0.2 mM phenylmethylsulfonyl fluoride by sonic oscillation. Membranes and debris were sedimented by centrifugation at 100,000 × *g* for 60 min. The fusion protein in the soluble fraction was purified by immunoglobulin G-Sepharose affinity chromatography (Pharmacia LKB Biotechnology), followed by preparative polyacrylamide gel electrophoresis (PAGE). The fusion protein was visualized by soaking the gel in 4 M sodium acetate (18). The appropriate band was excised, and protein was electroeluted into 25.6 mM Tris–192 mM glycine buffer (pH 8.4) and stored at −70°C. Rabbits were inoculated with 50 μg of protein in complete Freund adjuvant, followed by boosts of 50 μg in incomplete Freund adjuvant at 4- to 8-week intervals. Rabbits were bled at weekly intervals after the second and subsequent boosts.

Western blotting (immunoblotting). Cells were harvested from CF plates after development at 34°C by scraping with a razor blade in 0.2 ml of HM. Cells were frozen at −70°C until needed. Cells were resuspended in 10 mM HEPES buffer (pH 7.2) containing the following protease inhibitors: 5 mM EDTA, 0.5 μg of leupeptin per ml, 0.7 μg of pepstatin per ml, 1.0 mM *o*-phenanthroline, and 0.6 mM phenylmethylsulfonyl fluoride. Cells were then disrupted by sonication for 3 min on ice. The protein content of the extracts was determined with the BCA reagent (Pierce Chemical Co., Rockford, Ill.), and 10-μg samples were separated by PAGE. The running gel consisted of 11.56% acrylamide, 0.08% bisacrylamide, 380 mM Tris hydrochloride (pH 8.6), and 0.1% sodium dodecyl sulfate (SDS), the stacking gel consisted of 3.9% acrylamide, 0.06% bisacrylamide, 125 mM Tris hydrochloride (pH 6.8), and 0.1% SDS, and the running buffer consisted of 25.6 mM Tris–192 mM glycine (pH 8.4) containing 0.1% SDS. These conditions were chosen to optimize the separation of the modified forms of FrzCD. Fractionated proteins were transferred to nitrocellulose and stained with Ponceau S (44, 57). The blots were blocked with 10% dried milk in Tris-buffered saline (TBS; 50 mM Tris hydrochloride [pH 7.5], 150 mM NaCl) for 1 h at 24°C. Antiserum was added (1:400 dilution) and allowed to adsorb for an additional 1 to 2 h. Bound antibody was detected with ^{125}I-protein A (Amersham Corp., Arlington Heights, Ill.) or with the Amersham detection kit for rabbit antibodies (biotinylated donkey anti-rabbit antibody and streptavidin-linked alkaline phosphatase).

In vivo labeling and immunoprecipitation. Cells were harvested from CF agar after 14.5 h of development at 34°C and

diluted to a concentration of 2.5×10^9 cells in 0.5 ml of CF salts. Then 25 μCi of *S*-adenosyl-L-[*methyl*-^{3}H] methionine (^{3}H-SAM; 15 Ci/mmol) was added, and incubation was continued for 30 min. The cells were collected by centrifugation and solubilized by boiling for 3 min in 0.1 ml of TBS containing 1% SDS and the protease inhibitors listed above for 3 min at 100°C. The extracts were diluted with 0.9 ml of TBS containing 1% Triton X-100 and the protease inhibitors (TBSTi). Extracts were incubated with 20 μl of antisera for 2 h at 0°C, 200 μl of IgGsorb (The Enzyme Center, Malden, Mass.) was added, and incubation was continued for an additional 30 min. The immunoprecipitate was collected by centrifugation and washed four times with TBSTi and one time with TBS containing the protease inhibitors. The immunoprecipitate was solubilized by boiling for 3 min in protein loading buffer, and insoluble material was removed by centrifugation. Proteins were separated by PAGE as described above. Gels were stained with 0.05% Coomassie brilliant blue R in 25% isopropanol–10% acetic acid, destained in 10% acetic acid, soaked in Amplify (Amersham) for 30 min, and dried. Labeled bands were visualized by fluorography.

DNA sequencing. The DNA encoding *frzG* and *frzF* was subcloned into the vector pUC118 (59) from pBB12. A series of nested deletions was generated by using exonuclease III as described by Henikoff (15). Single-stranded templates from these deletions were prepared as described by Vieira and Messing (59). Double-stranded templates were isolated from *E. coli* DG98 and were prepared by the alkaline lysis procedure, followed by polyethylene glycol precipitation as described by Hattori and Sakaki (13). The strain from which the double-stranded plasmid templates were isolated was important; strains other than DG98 gave poor results. Both strands of the subcloned DNA were sequenced by the chain termination method of Sanger et al. (47) as modified by U.S. Biochemical Corp. (Cleveland, Ohio) for the modified T7 polymerase Sequenase, using [^{35}S]dATP (Amersham). When the endpoints of the nested deletions were separated by more than 250 bp, we used synthetic oligonucleotides as primers. The sequencing reactions were separated on 6% polyacrylamide gels containing 7 M urea and 40% (wt/vol) formamide to minimize gel artifacts due to the high G+C content of *M. xanthus*. Gels were soaked in 15% methanol–10% acetic acid for 30 min before drying. To sequence the sites of insertion of the Tn*5* mutations, we used a synthetic oligonucleotide primer homologous to Tn*5*. The plasmid DNAs containing Tn*5* insertions in which one of the IS*50*s had been deleted and which allowed sequencing with the synthetic oligonucleotide primers were constructed as previously described (4).

DNA and protein sequence analyses were performed with the DNA Inspector IIe (Textco, West Lebanon, N.H.) on a Macintosh Plus computer and with the Intelligenetics/BIONET programs. GenBank and NBRF data bases were searched by using the algorithms of Pearson and Lipman (40).

Photomicroscopy and time lapse videomicroscopy. Development was induced by spotting 5 μl of cells at 4×10^9 cells per ml onto CF plates solidified with 0.6% Gel Gro (ICN Biomedicals, Inc., Costa Mesa, Calif.) and maintained at 34°C. The plates were photographed by a Ricoh KR-10 Super camera attached to a Zeiss dissecting microscope.

The motility behavior of individual cells was examined at 23°C by spotting 5 μl of cells at 2×10^7 cells per ml onto a layer of CF agar on a microscope slide. The spot was allowed to dry for 15 min, after which an oxygen-permeable membrane (Yellow Springs Instrument Co., Inc., Yellow Springs, Ohio) was gently placed on top. The membrane maintained a flat surface, eliminated desiccation of the medium, and allowed an aerobic environment for extended periods of time. During the first hour after spotting, a large percentage of cells divide. Because motility behavior is altered preceding cell division (cells arrest their movement), we examined cells after this initial hour. Individual cell movements were examined and recorded by using a Zeiss microscope attached to a COHU camera (model 4815-2000/0000) and a JVC time lapse videorecorder (model BR-9000U).

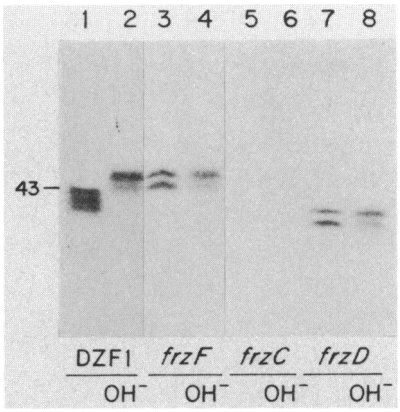

FIG. 2. Western immunoblot of FrzCD. Proteins in cell extracts were separated by SDS-PAGE and transferred onto nitrocellulose membranes. FrzCD was detected by using polyclonal antiserum and ^{125}I-protein A. To identify base-labile modifications, identical amounts of each sample were treated with 0.1 N NaOH for 30 min, followed by neutralization before running the gel (lanes 2, 4, 6, and 8). Lanes: 1 and 2, DZF1 (wild type); 3 and 4, DZF4023 (*frzF*); 5 and 6, DZF3401 (*frzC*); 7 and 8, DZF3460 (*frzD*).

RESULTS

Methylation of FrzCD. The sequence similarities between FrzCD and enteric MCPs (29) raise a number of interesting questions. Does FrzCD function as a receptor in a sensory transduction pathway controlling cell movements? If so, what stimulus or stimuli does it recognize? Is FrzCD reversibly methylated in vivo during adaptation to changing stimulus levels? To address some of these questions, we raised polyclonal antiserum against a protein A-FrzCD fusion protein. The antiserum recognized the *Salmonella typhimurium* MCP, Tar, in Western blots (data not shown). The antiserum also recognized a ladder of bands migrating between 44.5 and 41 kilodaltons (kDa) in extracts of wild-type *M. xanthus* cells (Fig. 2). These bands were in the approximate location predicted for FrzCD by sequence analysis (43.6 kDa; 29). These bands were not present in the *frzC* mutant DZF3401 (Fig. 2, lane 5), suggesting that the antiserum is specific for FrzCD. We tested the effect of mutations in various *frz* genes on the FrzCD banding pattern. Mutations in *frzA*, *frzB*, *frzE*, and *frzG* did not drastically alter the pattern of FrzCD bands observed (data not shown); however, minor differences in the intensities of the various bands were observed in these mutants. A strain with a Tn*5* mutation in *frzF*, DZF3593, drastically altered the pattern of FrzCD bands (lane 3). Instead of a series of bands migrating between 44.5 and 41 kDa, the *frzF* mutant produced two bands that migrated at 44.5 and 43 kDa.

The ladder of bands observed for wild-type cells is remi-

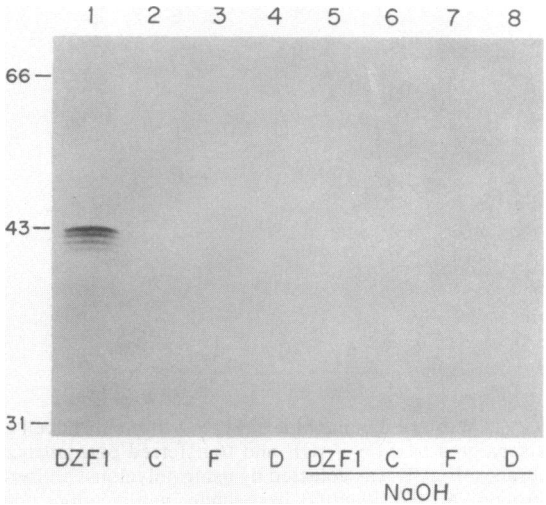

FIG. 3. In vivo methylation of FrzCD. Developmental cells were labeled with ^{3}H-SAM, after which FrzCD was immunoprecipitated. Half of each protein sample was treated with 0.1 N NaOH for 30 min and subsequently neutralized before being separated by SDS-PAGE. Labeled proteins were visualized by fluorography. Lanes: 1 and 5, DZF1 (wild type); 2 and 6, DZF3401 (*frzC*); 3 and 7, DZF4023 (*frzF*); 4 and 8, DZF3460 (*frzD*).

niscent of the pattern seen for methylated MCPs (49). MCPs contain multiple sites for reversible methylation of specific glutamate residues. The addition of each methyl group causes the MCP to migrate faster in the gel (8). Glutamate methyl esters are base labile (58). Treatment of wild-type *M. xanthus* extracts with 0.1 N NaOH chased the ladder of FrzCD bands into two slower-migrating bands that comigrated with the bands of the *frzF* mutant DZF3593. Base treatment of extracts of the *frzF* mutant did not alter the migration of the FrzCD bands. These data suggest that the multiple bands observed for FrzCD are the result of methylation and that *frzF* is required for methylation.

In a previous report, we predicted that the *frzD* mutant DZF3460 produces a truncated FrzCD protein with a calculated molecular weight of 38,700 (29). This prediction was confirmed (Fig. 2, lane 7), providing further evidence for the specificity of the antiserum. The migration of the truncated FrzCD protein produced by the *frzD* mutant was not altered by base treatment, suggesting that it was not methylated.

We assayed for methylation of FrzCD directly by in vivo labeling with ^{3}H-SAM. *M. xanthus*, unlike *S. typhimurium*, takes up SAM directly (36). Developing cells were harvested from solid CF medium and incubated in liquid CF with ^{3}H-SAM for 30 min. Labeled FrzCD was immunoprecipitated as described in Materials and Methods. After separation by PAGE, the gels were stained and labeled bands were visualized by fluorography (Fig. 3). A series of bands was observed in the Coomassie-stained gel which migrated at the same position as those observed by Western blot analysis (data not shown). Fluorography revealed that these bands had incorporated label from ^{3}H-SAM and that this label was not present in samples treated with 0.1 N NaOH before gel electrophoresis. Treatment with base caused a shift in the pattern of the Coomassie-stained bands similar to that observed by Western blot analysis: the ladder of bands was chased to two bands at 45 and 44 kDa. Neither the *frzC* mutant DZF3401, the *frzF* mutant DZF3593, nor the *frzD* mutant DZF3460 incorporated label into immunoprecipitable material migrating above the gel front (30 kDa). These data, which indicate that FrzCD is methylated and that this modification is dependent on *frzF*, prompted us to sequence *frzF*.

Nucleotide sequence of *frzG* and *frzF*. We determined the nucleotide sequence of the *frzF* complementation group. During a preliminary analysis of this sequence, we noted the presence of an open reading frame upstream of *frzF*, which prompted us to also subclone and sequence this region (*frzG*).

Previous complementation data (4) as well as maxicell analysis (6) indicated that the approximate sizes of *frzG* and *frzF* were 1.0 and 1.5 kbp, respectively. Open reading frame analysis revealed two reading frames of the appropriate sizes. The nucleotide sequence of *frzG* and *frzF* as well as the amino acid sequences of the predicted translation products are shown in Fig. 4. High-G+C organisms such as *M. xanthus* (67.5% G+C; 30) show a characteristic nucleotide bias at the three codon positions (3). The wobble position shows the highest percent G+C, the first position is intermediate, the middle position has the least percent G+C, usually around 50%. These reading frames exhibit the expected codon bias (Table 2).

Translational start sites within the correct reading frames were identified on the basis of earlier complementation data, the presence of possible initiation codons, appropriately spaced ribosome-binding sites, and homology to known genes (data presented below). The predicted initiation codon for the *frzG* peptide is located at nucleotide 120 of Fig. 4. Complementation data indicated that Tn*5* insert Ω226 lies outside of *frzE*. The site of insertion of this transposon (Fig. 4) is only 15 bp downstream from the stop codon of *frzE* (W. R. McCleary and D. R. Zusman, unpublished data). There are 31 bp between the end of Ω226 and the predicted initiation codon of *frzG*. The short distance between *frzE* and *frzG* supports the hypothesis proposed by Weinberg and Zusman (60) that the frizzy genes are part of a complex transcriptional unit with multiple promoters and polycistronic messages. We were unable to identify sequences that have been previously characterized as procaryotic promoters between *frzE* and *frzG* (14). Predicted ribosome-binding sites are underlined in Fig. 4. The sequences of the *M. xanthus* and *E. coli* 16S rRNAs are nearly identical in the region containing the Shine-Dalgarno complementary sequence (35), and sequences that have been predicted to function as ribosome-binding sites for other *M. xanthus* genes resemble *E. coli* Shine-Dalgarno sequences (19, 41, 51). The proposed *frzG* reading frame encodes a 334-amino-acid protein with a calculated molecular mass of 35,456 Da (Fig. 4). This size is in close agreement to the one estimated from SDS-polyacrylamide gels of labeled proteins from *E. coli* maxicells expressing *frzG* (6).

There are two possible initiation codons for *frzF* (Fig. 4). The first, located at position 1116, is a GTG and overlaps the stop codon of *frzG* by seven nucleotides. This configuration would couple *frzF* translation to that of *frzG*. Translational coupling has been hypothesized to be one scheme that allows equimolar translation of adjacent genes from polycistronic messages (34). The second potential start codon, an ATG, is located 120 bp downstream, at position 1235. Tn*5* Ω243, mapping in *frzG*, lies 5′ to both of the possible start sites. Within the 120 bp between the two potential start codons there are two short A+T-rich regions, separated by 39 bp. The first is 63% A+T over 19 bases; the other is 50% A+T over 20 bases. The calculated molecular weight of the 593-amino-acid peptide initiated from the upstream GTG is 64,562, whereas the 554-amino-acid peptide initiated from

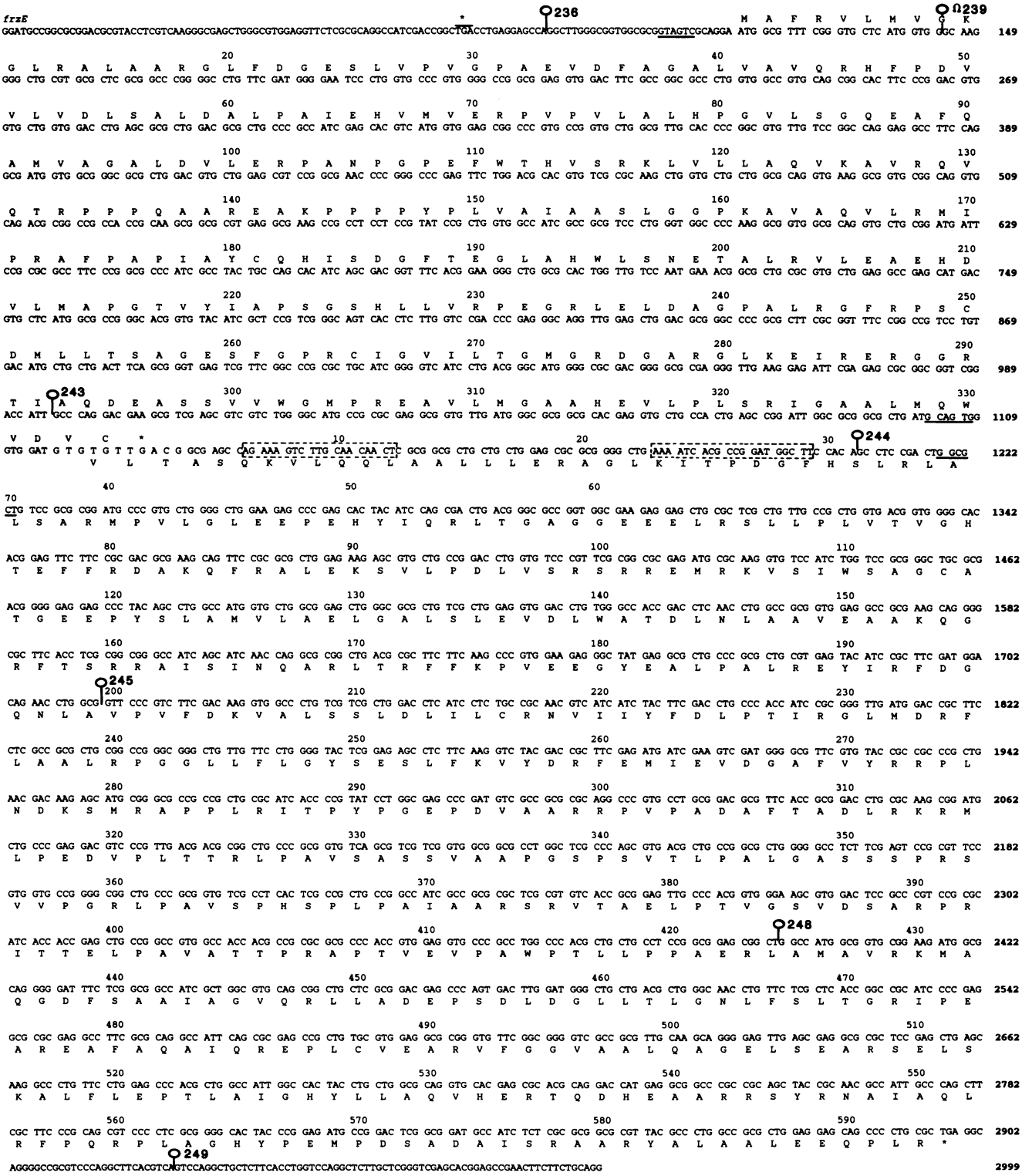

FIG. 4. Nucleotide and predicted amino acid sequences of *M. xanthus frzG* and *frzF* (GenBank accession no. M35200). The stop codons for *frzE*, *frzG*, and *frzF* are identified by an asterisk above the coding region. The predicted ribosome-binding sequences are underlined. The right end of each Tn*5* insertion is identified by ♀. The two short A+T-rich stretches in the 5′ region of *frzF* are boxed.

the downstream ATG has a predicted molecular weight of 60,385. Maxicell analysis in *E. coli* of a plasmid containing the entire *frz* region transcribed from an inducible promoter indicated that *frzF* produced a protein with an apparent molecular weight of 54,000 (6). However, we feel that the maxicell data are insufficient to distinguish between the two possible start sites because the size of the protein produced in *E. coli* cells may not correspond to that produced in *M. xanthus*, since *E. coli* and *M. xanthus* may recognize different translational start sites and there is considerable

TABLE 2. Percentage G+C at codon positions in *frz* open reading frames

Open reading frame	% G+C at codon position:		
	1	2	3
frzG	75	49	89
frzF	71	49	92

variability in the way proteins of a given molecular weight run on polyacrylamide gels.

Sequence similarities between FrzF and CheR and between FrzG and CheB. The putative *frzF* gene product has a large N-terminal domain that shows 31% sequence identity (83 of 271 amino acids) to the *cheR* methyltransferase of *E. coli* (32) (Fig. 5). The region of homology spans the entire CheR protein. If we assume that translation is initiated at the GTG codon at position 1116, then the sequence similarity between FrzF and CheR starts at residue 2 of FrzF. It is because of this amino acid sequence similarity that we have designated this codon as the putative translational initiation site. The region of sequence similarity between the two potential translational start sites is boxed in Fig. 5.

Because strains with Tn*5* mutations in the 1-kbp gap region that separates *frzE* from *frzF* are fruiting proficient, we were surprised to learn that the putative *frzG* protein has significant sequence similarity to CheB of *E. coli* (32) (Fig. 6). CheB is the chemotactic methylesterase that acts on the MCPs during the adaptive response (55). In addition to demethylating MCPs, this enzyme deamidates several glutaminyl residues of the MCPs, which are subsequently available for methylation. FrzG shows 31% amino acid identity (105 of 334 residues) with CheB. There are also numerous conservative substitutions throughout this alignment. The amino-terminal domain of CheB is a regulatory region that is modulated by CheA (27); this domain is homologous to CheY (56). Figure 6 also shows the alignment of FrzG to CheY. There is only 19% amino acid identity between the conserved regions of FrzG and the entire CheY sequence. CheY and CheB are members of a conserved family of bacterial response modulator proteins. There are five residues that are almost entirely conserved throughout this family. In reference to CheY, they are Asp-13, Asp-57, Gly-102, Ala-103, and Lys-109. The crystal structure of CheY has been solved and shows that the three highly conserved charged residues are clustered on one surface of the protein (53). Of these five highly conserved residues, only Asp-57, Gly-102, and Ala-103 are conserved between CheY and FrzG. Regions of hydrophobic residues thought to be important in maintaining secondary structure are also conserved.

Reevaluation of the FrzG phenotype. The similarity of FrzG to enteric CheB prompted us to evaluate the effect of *frzG* mutations on FrzCD, on the motility behavior of individual cells, and on the aggregation and fruiting behavior of swarms. The added resolution gained by staining Western immunoblots with streptavidin alkaline phosphatase allowed us to distinguish subtle differences between the wild type and several mutants in the FrzCD banding patterns (Fig. 7). As mentioned above, FrzCD from extracts of wild-type *M. xanthus* migrated as a ladder of bands. In Fig. 2 we observed a 44.5-kDa band from extracts of *frzF*. The streptavidin alkaline phosphatase staining resolved this band into two bands (45 and 44 kDa). This doublet was also evident in overexposed Western immunoblots from extracts of wild-type cells. The 43-kDa band, which we believe was a proteolytic fragment, was not predominant in this experiment. Sequence similarities reported above suggested that

FIG. 5. Comparison of the deduced amino acid sequences of *M. xanthus* FrzF and *E. coli* CheR. Regions of amino acid identity are boxed with solid lines. Numbering starts at the N terminus of each protein. The dashed-line box indicates the predicted FrzF translation product between the two potential start codons.

```
FrzG  MAFRVLMVGKG--LRALAARGLFDGESLVPVGPAEVDFAG   38
CheB  SKIRVLSVDDSALMRQIMTEIINSHSDMEMVATAP-DPLV   40
CheY  KELKFLVVDDFSTMRRIVRNLLKEL-GFNNVEEAE-DGVD   41

FrzG  ALVAVQRHFPDVVLVDLSA--LDALPAIEHVMVERPVP--   74
CheB  ARDLIKKFNPDVLTLDVEMPRMDGLDFLEKLMRLRPMPVV   80
CheY  ALNKLGAGGYGFVISDWNMPNMDGLELLKTIRADGAMSAL   81

FrzG  VLALHPGVLSGQEAFQAMVAGALDVLERPANPGPEG----  110
CheB  MVSSLTGKGS-EVTLRALELGAIDFVTKPQLGIREGMLAY  119
CheY  PVLMVTAEAKKENIIAAAQAGASGYVVKPFTAATLEEKLN  121

FrzG  WTHVSRKLVLLAQVKAVRQVQTRPPPQAAREAKPPPPYPL  150
CheB  NEMIAEKVRTAAKASLAAHKPLSAPTTLKAGPLLSS-EKL  158
CheY  KIFEKLGM                                 129

FrzG  VAIAASLGGPKAVAQVLRMIPRAFPAP-IAYCQHISDGFT  189
CheB  IAIGASTGGTEAIRHVI--QPLPLSSPALLITQHMPPGFT  196

FrzG  EGLAHWLSNETALRVLEAEHDVLMAPGTVYIAPSGSHLLV  229
CheB  RSFADRLNKLCQIGVKEAEDGERVLPGHAYIAPGDRHMEL  236

FrzG  PPEG---RLELDAGPALRGFRPFCAMLLTSAGESFGPRCI  266
CheB  SRSGANYQIKIHDGPAVNRHRPSVDVLFHSVAKQAGRNAV  276

FrzG  GVILTGMGRDGARGLKEIRERGGRTIAQDEASSVVWGMPR  306
CheB  GVILTGMGNDGAAGMLAMRQAGAWTLAQNEASCVVFGMPR  316

FrzG  EAVLMGAAHEVLPLSRIGAALMQWVDVC              334
CheB  EAINMGGVCEVVDLSQVSQQMLAKISAGQAIRI         349
```

FIG. 6. Comparison of the deduced amino acid sequences of *M. xanthus* FrzG and *E. coli* CheB and CheY. Regions of amino acid identity are boxed. Numbering starts at the N terminus of each protein.

frzG encoded a protein methylesterase or deamidase. In the absence of FrzG, we would expect to observe a ladder of bands extending from the unmodified protein band down to the fully methylated form. This was observed; furthermore, the bands were chased by NaOH treatment to the position of the slowest-migrating bands, which indicated that FrzCD was methylated. The uppermost band from the *frzG* extracts migrated at 44 kDa. We believe that this is the unmodified form of FrzCD and that the 45-kDa band is the result of a specific deamidation catalyzed by *frzG*.

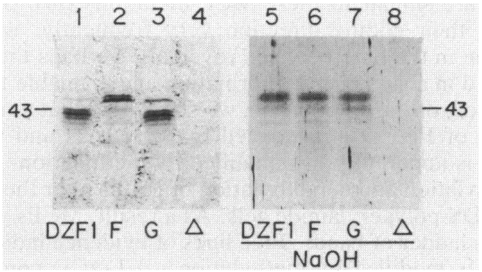

FIG. 7. Western immunoblot of FrzCD showing the effects of a *frzG* mutation. Cell extracts of DZF1 (lanes 1 and 5), *frzF* (lanes 2 and 6), *frzG* (lanes 3 and 7), and a deletion strain lacking *frzCD* (DZF3558) (lanes 4 and 8) were separated by SDS-PAGE and transferred onto nitrocellulose. Proteins were detected with polyclonal rabbit antiserum to a protein A-FrzCD fusion protein and a biotinylated anti-rabbit antibody–streptavidin-linked alkaline phosphatase detection kit. Identical amounts of each sample were treated with 0.1 N NaOH for 30 min and neutralized before electrophoresis.

Since *frz* mutations alter the gliding behavior of individual cells, we were interested in determining the effects of a *frzG* mutation on gliding. Vegetatively growing cells were harvested by centrifugation, diluted, and spotted onto a layer of CF agar on a microscope slide as described in Materials and Methods. The motility behaviors of individual cells were recorded by time lapse videomicroscopy (Table 3). At low

TABLE 3. Frequency of cell reversal in wild-type and *frz* mutants

Strain	Genotype	No. of cells observed	No. of reversals/cell per h (mean ± SD)
DZF1	*frz*$^+$	26	8.1 ± 2.1
DZF3460	*frzD*	27	31.7 ± 5.4
DZF4021	*frzG*	29	13.9 ± 5.7
DZF4023	*frzF*	28	2.0 ± 2.4

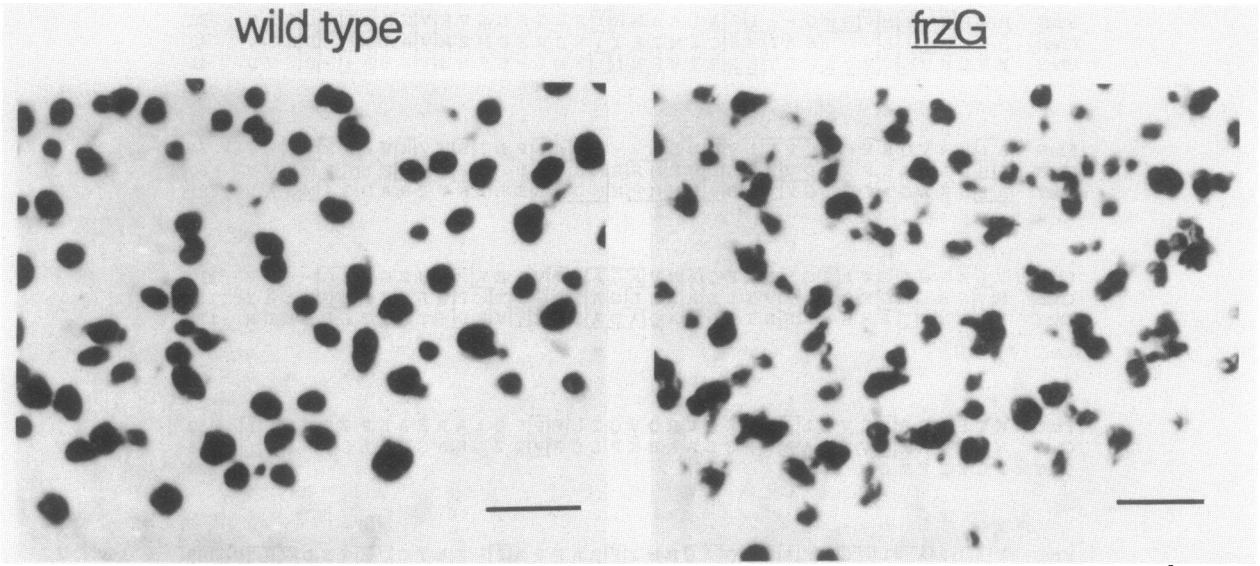

FIG. 8. Reexamination of the *frzG* phenotype. Vegetative cells of DZF1 and the *frzG* mutant were concentrated to 4×10^9 cells per ml, spotted onto CF plates, and photographed after 48 h of development. Bar, 0.5 mm.

cell density, wild-type cells reversed their gliding direction, on average, 8.1 times per h. In contrast, *frzF* mutants reversed very infrequently (less than 2 times per h), whereas *frzG* and *frzD* mutants reversed more frequently than wild type (13.9 and 31.7 times per h, respectively).

The region that we have called *frzG* was originally designated gap because strains containing Tn*5* insertions in this region formed fruiting bodies. In light of the evidence described above, we reexamined the fruiting behavior of these mutants. The results (Fig. 8) indicate that fruiting body formation is subtly impaired in *frzG* mutants. In comparison to DZF1 fruiting bodies, which are glossy and have rounded, even edges, *frzG* fruiting bodies are smaller, are rough in appearance, and have irregular edges.

DISCUSSION

The *frz* genes of *M. xanthus* are required for the normal aggregation of cells during fruiting body formation. In this report, we provide further support for the hypothesis that the *frz* genes constitute a sensory transduction pathway that controls the frequency at which cells reverse their gliding direction. With the characterization of *frzG* and *frzF* presented here, we have now analyzed DNA sequences that encode five components of this pathway. Four of the components, FrzA, FrzCD, FrzG, and FrzF, show homology to CheW, the MCPs, CheB, and CheR, respectively, of the enteric chemotactic signal transduction pathway. In addition, we have recently sequenced the *frzE* gene of *M. xanthus* and found that the deduced protein product has domains that are homologous to both CheA and CheY (McCleary and Zusman, unpublished data). The *che* genes control the swimming behavior of individual cells by adjusting the frequency at which flagella reverse their direction of rotation in response to chemoeffectors (28). We propose that the *frz* sensory transduction pathway similarly controls the gliding behavior of individual cells by adjusting the frequency at which cells reverse direction in response to external stimuli, e.g., aggregation or feeding signals.

In enterobacterial chemotaxis, MCPs transmit their ligand occupancy status to the flagella by means of a phosphorylation cascade involving CheW, CheA, and CheY (37). CheY-phosphate is the response regulator that interacts directly with the flagellar switch and controls the direction of flagellar rotation, causing the cell to run or tumble. The cell gradually adapts to the new level of stimulus and returns to prestimulus levels of runs and tumbles. This adaptation involves methylation and demethylation of the MCPs catalyzed by CheR and CheB, respectively.

Evidence presented in this report adds support to the hypothesis, generated from sequence analysis, that the function of FrzCD in the *frz* sensory transduction pathway is similar to that of the MCPs in chemotaxis. The signaling ability of MCPs appears to be highly dependent on the conformation of the signaling domain (1). It is thought that alterations in this conformation brought about by interactions of the periplasmic domain with chemoeffectors and other binding proteins, by covalent modifications of glutamyl residues flanking the signaling domain, or by mutation alter the signaling status of the molecule. Mutations that cause the production of truncated MCPs often result in a dominant phenotype in which the cells are unable to adapt (1, 23, 43). These truncated MCPs appear to be locked in a particular signaling mode. We hypothesized previously that *frzD* mutations are similar to these MCP mutations (29). *frzD* cells reverse their gliding direction very frequently, with little variation in the time between reversals. Perhaps the protein is locked in a signaling conformation and is unable to adapt. In support of this hypothesis, we show here that a truncated version of FrzCD is produced by *frzD* cells and that this protein is apparently not modified by methylation.

Methylation and demethylation of MCPs alter their mobility in SDS-polyacrylamide gels. As a result, MCPs generally run as a ladder of bands. Five lines of evidence indicate that FrzCD is modified by methylation. (i) FrzCD contains regions similar in sequence to the methylatable sites of the MCPs. (ii) FrzCD migrates as a ladder of bands between 45 and 41 kDa. (iii) Glutamate methyl esters are base labile. Treatment of cell extracts with alkali before electrophoresis chased the ladder into a set of bands that migrated more slowly. A similar shift toward higher apparent molecular weight is observed when enteric MCPs undergo demethylation and deamidation. (iv) A ladder of radiolabeled FrzCD

bands was detected when developing *M. xanthus* cells were labeled with the methyl donor ^{3}H-SAM. (v) Mutants of the putative methyltransferase, *frzF*, failed to produce the modified forms of FrzCD.

The *frzF* gene encodes a protein whose N-terminal region is homologous to the sequence of entire enteric methyltransferase CheR. The C-terminal half of the protein is not similar to any known chemotaxis protein; we do not yet know its function, nor do we know which of the two possible translational start sites observed for *frzF* is utilized. Homology data supports the upstream GTG start site. However, the following lines of evidence support the downstream ATG start site. Between the two potential start sites there are two 20-bp A+T-rich patches separated by 39 bp which may be associated with the regulatory functions that are often found 5′ to structural genes. Tn*5* insertions in *frzG*, including Ω243, which is 138 bp upstream of the A+T-rich region, apparently do not eliminate *frzF* expression, since FrzCD is still modified in these mutants (Fig. 8). This observation supports the hypothesis that this A+T-rich region contains a promoter. Finally, codon usage tables from previously sequenced *M. xanthus* genes (12, 19, 41) indicate that these two A+T-rich patches consist of rare codons, which may indicate that translation from the upstream site is unlikely. However, if the protein is translated from this upstream site, these rare codons may be important in the regulation of its expression. The two translation start sites are not mutually exclusive and might provide another regulatory mechanism for the expression of this gene. Under some conditions it might be useful to couple translation of FrzF to FrzG, whereas at other times independent expression would be beneficial.

The gap region between *frzE* and *frzF* was originally identified because cells with Tn*5* mutations in this region were not *frz*. These mutants were able to form fruiting bodies. Sequence analysis indicated that this region encodes a protein homologous over its entire length to CheB, the chemotactic methylesterase. For this reason, the gap is now designated *frzG*.

CheB is made up of an N-terminal regulatory domain and a C-terminal catalytic domain containing the methylesterase activity. Preliminary work with inhibitors indicated that CheB was a thiol esterase (48). However, a more recent analysis using site-specific mutagenesis has demonstrated that this is not the case (J. K. Krueger, A. M. Stock, C. E. Schutt, and J. B. Stock., *in AAAS Symposium on Protein Folding*, in press). There are two cysteinyl residues in the catalytic domain of CheB. A mutant was engineered that exchanged both cysteines for serines; this enzyme retained catalytic activity. If, as we predict, *frzG* encodes a methylesterase similar to CheB, then it is likely that the active-site residues are conserved between CheB and FrzG. Neither of the cysteine residues found in the catalytic domain of CheB are conserved in FrzG. This finding supports the hypothesis that CheB is not a thiol esterase.

The N-terminal regulatory domain of CheB has a structural motif found in a large family of response regulator proteins (CheY, NtrC, CheB, Spo0F, OmpR, etc.) for which CheY is the paradigm (56). The regulatory domain of CheB (like that of CheY) is phosphorylated by its cognate kinase, CheA, in a feedback loop that increases its ability to demethylate the MCPs. This feedback loop confers an asymmetry to the chemotactic response by decreasing tumbling times in relationship to smooth swimming (22). The phosphorylated residue in CheY-phosphate is Asp-57 (45). The crystal structure of CheY has been solved and demonstrates that this protein is an α/β structure (53). The sequence similarity between FrzG and CheY conserves the hydrophobic stretches thought to be important for maintaining secondary structure as well as most of the highly conserved amino acid residues found in this family of proteins. Significant differences are found at two sites of the regulatory domain; in reference to CheY, FrzG contains a lysine in place of Asp-13 and an arginine in place of Lys-109. FlbD from *Caulobacter crescentus*, a homolog to NtrC and an activator of σ^{54}-dependent flagellar gene expression, shows the same Lys-for-Asp substitution as well as a Leu-for-Lys substitution at position 109 (G. Ramakrishnan and A. Newton, Proc. Natl. Acad. Sci. USA, in press). The conserved sequence motifs between FrzG and CheB suggest a conserved structure and function and allow us to speculate that FrzG is regulated by its cognate kinase, FrzE (McCleary and Zusman, unpublished data).

When we reexamined the phenotype of *frzG* mutants, we discovered that although these mutants appear very similar to wild-type *M. xanthus* under fruiting conditions, there are subtle yet significant differences. The fruiting bodies formed by *frzG* cells were on average smaller and appeared irregular and sloppy. Perhaps adaptation to aggregation signals during fruiting body morphogenesis was impaired. Time lapse videomicroscopy showed that on average *frzG* cells reversed their direction of movement twice as often as did wild-type cells. This phenotype is somewhat similar to the tumbly behavior of *cheB* mutants in the absence of stimuli. The MCPs from *cheB* cells are highly methylated and constantly signal the flagella to rotate clockwise, thereby generating tumbles. There was some variation in the motility pattern of individual *frzG* cells, as indicated by the large standard deviation in the reversals per hour. Twenty-four of the cells reversed direction frequently (15.8 ± 3.6 reversals per cell per h), whereas four of the cells moved with long episodes of unidirectional movement (1.2 reversals per cell per h). This behavior is reminiscent of *cheB* cells, which are tumbly in the absence of stimuli but swim smoothly for extended periods after exposure to saturating changes in chemoeffector concentrations because they are unable to adapt (54). In Western immunoblots from *frzG* extracts, the absence of the uppermost FrzCD band at 45 kDa (postulated to be a deamidated form of the unmethylated protein) suggests that *frzG* encodes a protein with deamidase activity. A summation of the evidence from mutant analysis indicates that the unmodified form of FrzCD migrates at 44 kDa, a deamidated form migrates at 45 kDa, and the methylated forms migrate between 44 and 41 kDa.

In our current working model, the *frz* sensory transduction pathway consists of a signaling protein, FrzCD, which is covalently modified to mediate adaptation. The enzymes responsible for the modifications, methylation and demethylation, are FrzF and FrzG, respectively. In analogy to the chemotaxis system, FrzCD probably interacts with FrzE (McCleary and Zusman, unpublished data) by means of FrzA. We hypothesize that FrzE interacts either directly or indirectly with components of the gliding machinery that determine reversal frequency. Genetic and biochemical experiments based on these assumptions should bring considerable insight into the mechanisms of gliding motility.

Because of the evolutionary distance between the enteric bacteria and the myxobacteria and the many differences in their physiology and life cycles, we feel that comparative analysis of the *frz* and *che* systems will provide insight into the essential components and principles of bacterial sensory transduction. Among the many differences between the *E. coli* and *M. xanthus* systems of movement and directional

control (movement in three dimensions as opposed to two; random redirection by Brownian motion versus redirection by inconsistencies of the surface on which the cells glide), perhaps the most striking is the difference in the time scales over which excitation and adaptation must take place in each system. *E. coli* moves at a rate of approximately 1,500 μm/min (2). Adapted cells punctuate their runs approximately every 1 to 2 s with a 0.1- to 0.2-s tumble. Excitation occurs in less than 1 s after exposure to a chemoeffector, and adaptation follows this over a period of seconds to minutes. In contrast, *M. xanthus* cells move at approximately 2 μm/min and change direction approximately every 7 to 8 min (5). If a proportional reduction occurs in the speed of excitation and adaptation, some aspects of the molecular details of signal transduction may be more easily studied in the myxobacteria.

How are the signals that coordinate developmental aggregation conveyed to individual cells in a feeding swarm? What is the nature of these signals and how are they processed? Dworkin and Eide (10) were unable to provide evidence for chemotaxis of *M. xanthus* cells toward a variety of compounds. They hypothesized that it is unlikely that such slow-moving cells could respond to a concentration gradient of a freely diffusible compound by using a temporal sensing mechanism such as that used by the enteric bacteria. While taxis toward a freely diffusible molecule may be unlikely, myxobacterial cells may respond to signals which diffuse slowly along a solid surface or through the myxobacterial slime layer. Alternatively, cells may respond to signals that remain bound to cell surfaces or to the substratum. The social nature of the myxobacterial life cycle involving repeated cell contacts makes this an attractive idea. We hope that further study of the *frz* genes and gene products will provide some insight into the nature of these intercellular signals.

ACKNOWLEDGMENTS

We thank Kathleen O'Connor, Joe Romeo, Kathy Trudeau, and Robin Weinberg for helpful discussions. We thank Jeff Stock and Austin Newton for providing information prior to publication. We also thank the Animal Support Facility at the University of California, Berkeley, for assistance with animal procedures.

This research was supported by Public Health Service grant GM 20509 from the National Institutes of Health and grant DMB-8820799 from the National Science Foundation. M.J.M. was supported by Public Health Service postdoctoral fellowship GM 12356 from the National Institutes of Health. W.R.M. was the recipient of National Research Service Award traineeship GM 07232-12 from the National Institutes of Health.

LITERATURE CITED

1. **Ames, P., and J. S. Parkinson.** 1988. Transmembrane signaling by bacterial chemoreceptors: *E. coli* transducers with locked signal output. Cell **55**:817–826.
2. **Berg, H. C., and D. A. Brown.** 1972. Chemotaxis in *Escherichia coli* analyzed by three-dimensional tracking. Nature (London) **239**:500–504.
3. **Bibb, M. J., P. R. Findlay, and M. W. Johnson.** 1984. The relationship between base composition and codon usage in bacterial genes and its use for the simple and reliable identification of protein coding sequences. Gene **30**:157–166.
4. **Blackhart, B. D., and D. R. Zusman.** 1985. Cloning and complementation analysis of the "frizzy" genes of *Myxococcus xanthus*. Mol. Gen. Genet. **198**:243–254.
5. **Blackhart, B. D., and D. R. Zusman.** 1985. "Frizzy" genes of *Myxococcus xanthus* are involved in control of frequency of reversal of gliding motility. Proc. Natl. Acad. Sci. USA **82**: 8767–8770.
6. **Blackhart, B. D., and D. R. Zusman.** 1986. Analysis of the products of the *Myxococcus xanthus frz* genes. J. Bacteriol. **166**:673–678.
7. **Campos, J. M., J. Geisselsoder, and D. R. Zusman.** 1978. Isolation of bacteriophage MX4, a generalized transducing phage from *Myxococcus xanthus*. J. Mol. Biol. **119**:167–178.
8. **Defranco, A. L., and D. E. Koshland, Jr.** 1980. Multiple methylation in processing of sensory signals during bacterial chemotaxis. Proc. Natl. Acad. Sci. USA **77**:2429–2433.
9. **Dworkin, M.** 1962. Nutritional requirements for vegetative growth of *Myxococcus xanthus*. J. Bacteriol. **84**:250–257.
10. **Dworkin, M., and D. Eide.** 1983. *Myxococcus xanthus* does not respond chemotactically to moderate concentration gradients. J. Bacteriol. **154**:437–442.
11. **Hagen, D. C., A. P. Bretscher, and D. Kaiser.** 1978. Synergism between morphogenetic mutants of *Myxococcus xanthus*. Dev. Biol. **64**:284–296.
12. **Hagen, T. J., and L. J. Shimkets.** 1990. Nucleotide sequence and transcriptional products of the *csg* locus of *Myxococcus xanthus*. J. Bacteriol. **172**:15–23.
13. **Hattori, M., and Y. Sakaki.** 1986. Dideoxy sequencing method using denatured plasmid templates. Anal. Biochem. **152**:232–238.
14. **Helmann, J. D., and M. J. Chamberlin.** 1988. Structure and function of bacterial sigma factors. Annu. Rev. Biochem. **57**: 839–872.
15. **Henikoff, S.** 1984. Unidirectional digestion with exonuclease III creates targeted breakpoints for DNA sequencing. Gene **28**:351–359.
16. **Hess, J. F., K. Oosawa, N. Kaplan, and M. I. Simon.** 1988. Phosphorylation of three proteins in the signaling pathway of bacterial chemotaxis. Cell **53**:79–87.
17. **Hess, J. F., K. Oosawa, P. Matsumura, and M. I. Simon.** 1987. Protein phosphorylation is involved in bacterial chemotaxis. Proc. Natl. Acad. Sci. USA **84**:7609–7613.
18. **Higgins, R. C., and M. E. Dahmus.** 1979. Rapid visualization of protein bands in preparative SDS-polyacrylamide gels. Anal. Biochem. **93**:257–260.
19. **Inouye, S., T. Franceschini, and M. Inouye.** 1983. Structural similarities between the development-specific protein S from a gram-negative bacterium, *Myxococcus xanthus*, and calmodulin. Proc. Natl. Acad. Sci. USA **80**:6829–6833.
20. **Keller, K. H., M. Grady, and M. Dworkin.** 1983. Surface tension gradients: feasible model for gliding motility in *Myxococcus xanthus*. J. Bacteriol. **155**:1358–1366.
21. **Koshland, D. E., Jr.** 1981. Biochemistry of sensing and adaptation in a simple bacterial system. Annu. Rev. Biochem. **50**:765–782.
22. **Koshland, D. E., Jr., D. A. Sanders, and R. M. Weis.** 1988. Roles of methylation and phosphorylation in the bacterial sensing system. Cold Spring Harbor Symp. Quant. Biol. **53**:11–17.
23. **Krikos, A., M. P. Conley, A. Boyd, H. C. Berg, and M. I. Simon.** 1985. Chimeric chemosensory transducers of *Escherichia coli*. Proc. Natl. Acad. Sci. USA **82**:1326–1330.
24. **Kuspa, A., and D. Kaiser.** 1989. Genes required for developmental signaling in *Myxococcus xanthus*: three *asg* loci. J. Bacteriol. **171**:2762–2772.
25. **Lapidus, I. R., and H. C. Berg.** 1982. Gliding motility of *Cytophaga* sp. strain U67. J. Bacteriol. **151**:384–398.
26. **Liu, J., and J. S. Parkinson.** 1989. Role of CheW protein in coupling membrane receptors to the intracellular signaling system of bacterial chemotaxis. Proc. Natl. Acad. Sci. USA **86**:8703–8707.
27. **Lupas, A., and J. Stock.** 1989. Phosphorylation of an N-terminal regulatory domain activates the CheB methylesterase in bacterial chemotaxis. J. Biol. Chem. **264**:17337–17342.
28. **Macnab, R. M.** 1987. Motility and chemotaxis, p. 732–759. *In* F. C. Neidhardt, J. L. Ingraham, K. B. Low, B. Magasanik, M. Schaechter, and H. E. Umbarger (ed.), *Escherichia coli* and *Salmonella typhimurium*: cellular and molecular biology. American Society for Microbiology, Washington D.C.
29. **McBride, M. J., R. A. Weinberg, and D. R. Zusman.** 1989. "Frizzy" aggregation genes of the gliding bacterium *Myxococ-*

cus xanthus show sequence similarities to the chemotaxis genes of enteric bacteria. Proc. Natl. Acad. Sci. USA **86**:424–428.
30. **Mesbah, M., U. Premachandran, and W. B. Whitman.** 1989. Precise measurement of the G+C content of deoxyribonucleic acid by high-performance liquid chromatography. Int. J. Syst. Bacteriol. **39**:159–167.
31. **Morrison, C. E., and D. R. Zusman.** 1979. *Myxococcus xanthus* mutants with temperature-sensitive, stage-specific defects: evidence for independent pathways in development. J. Bacteriol. **155**:317–329.
32. **Mutoh, N., and M. I. Simon.** 1986. Nucleotide sequence corresponding to five chemotaxis genes in *Escherichia coli*. J. Bacteriol. **165**:161–166.
33. **O'Connor, K., and D. R. Zusman.** 1983. Coliphage P1-mediated transduction of cloned DNA from *Escherichia coli* to *Myxococcus xanthus*: use for complementation and recombinational analyses. J. Bacteriol. **155**:317–329.
34. **Oppenheim, S. D., and C. Yanofsky.** 1980. Translational coupling during expression of the tryptophan operon of *Escherichia coli*. Genetics **95**:785–795.
35. **Oyaizu, H., and C. R. Woese.** 1985. Phylogenetic relationships among the sulfate respiring bacteria, myxobacteria and purple bacteria. Syst. Appl. Microbiol. **6**:257–263.
36. **Panesenko, S. M.** 1985. Methylation of macromolecules during development in *Myxococcus xanthus*. J. Bacteriol. **164**:495–500.
37. **Parkinson, J. S.** 1988. Protein phosphorylation in bacterial chemotaxis. Cell **53**:1–2.
38. **Parkinson, J. S., S. R. Parker, P. B. Talbert, and S. E. Houts.** 1983. Interactions between chemotaxis genes and flagellar genes in *Escherichia coli*. J. Bacteriol. **155**:265–274.
39. **Pate, J. L., and L. Y. E. Chang.** 1979. Evidence that gliding motility in prokaryotic cells is driven by rotary assemblies in the cell envelopes. Curr. Microbiol. **2**:59–64.
40. **Pearson, W. R., and D. J. Lipman.** 1987. Improved tools for biological sequence comparison. Proc. Natl. Acad. Sci. USA **85**:2444–2448.
41. **Romeo, J. M., B. Esmon, and D. R. Zusman.** 1986. Nucleotide sequence of the myxobacterial hemagglutinin gene contains four homologous domains. Proc. Natl. Acad. Sci. USA **83**:6332–6336.
42. **Rosenberg, E.** 1984. Myxobacteria: development and cell interactions. Springer-Verlag, New York.
43. **Russo, A. F., and D. E. Koshland, Jr.** 1983. Separation of signal transduction and adaptation functions of the aspartate receptor in bacterial sensing. Science **220**:1016–1020.
44. **Salinovich, O., and R. Montelaro.** 1986. Reversible staining and peptide mapping of proteins transferred to nitrocellulose after separation by SDS-PAGE. Anal. Biochem. **156**:341–347.
45. **Sanders, D. A., B. L. Gillece-Castro, A. M. Stock, A. L. Burlingame, and D. E. Koshland, Jr.** 1989. Identification of the site of phosphorylation of the chemotaxis response regulator protein, CheY. J. Biol. Chem. **264**:21770–21778.
46. **Sanders, D. A., B. Mendez, and D. E. Koshland, Jr.** 1989. Role of the CheW protein in bacterial chemotaxis: overexpression is equivalent to absence. J. Bacteriol. **171**:6271–6278.
47. **Sanger, F., S. Nicklen, and A. R. Coulson.** 1977. DNA sequencing with chain-terminating inhibitors. Proc. Natl. Acad. Sci. USA **74**:5463–5467.
48. **Simms, S. A., E. W. Cornman, J. Mottonen, and J. Stock.** 1987. Active site of the enzyme which demethylates receptors during bacterial chemotaxis. J. Biol. Chem. **262**:29–31.
49. **Springer, M. S., M. F. Goy, and J. Adler.** 1977. Sensory transduction in *Escherichia coli*: two complementary pathways of information processing that involve methylated proteins. Proc. Natl. Acad. Sci. USA **74**:3312–3316.
50. **Springer, W. R., and D. E. Koshland, Jr.** 1977. Identification of a protein methyltransferase as the *cheR* gene product in the bacterial sensing system. Proc. Natl. Acad. Sci. USA **74**:533–537.
51. **Stephens, K., P. Hartzell, and D. Kaiser.** 1989. Gliding motility in *Myxococcus xanthus*: *mgl* locus, RNA, and predicted protein products. J. Bacteriol. **171**:819–830.
52. **Stewart, R. C., and F. W. Dahlquist.** 1987. Molecular components of bacterial chemotaxis. Chem. Rev. **87**:997–1025.
53. **Stock, A. M., J. M. Mottonen, J. B. Stock, and C. E. Schutt.** 1989. Three-dimensional structure of CheY, the response regulator of bacterial chemotaxis. Nature (London) **337**:745–749.
54. **Stock, J., G. Kersulis, and D. E. Koshland, Jr.** 1985. Neither methylating nor demethylating enzymes are required for bacterial chemotaxis. Cell **42**:683–690.
55. **Stock, J. B., and D. E. Koshland, Jr.** 1978. A protein methylesterase involved in bacterial sensing. Proc. Natl. Acad. Sci. USA **75**:3659–3663.
56. **Stock, J. B., A. J. Ninfa, and A. M. Stock.** 1989. Protein phosphorylation and regulation of adaptive responses in bacteria. Microbiol. Rev. **53**:450–490.
57. **Towbin, H., T. Staehelin, and J. Gordon.** 1979. Electrophoretic transfer of proteins from polyacrylamide gels to nitrocellulose sheets: procedure and some applications. Proc. Natl. Acad. Sci. USA **76**:4350–4354.
58. **Van der Werf, P., and D. E. Koshland, Jr.** 1977. Identification of a γ-glutamyl methyl ester in bacterial membrane protein involved in chemotaxis. J. Biol. Chem. **252**:2793–2795.
59. **Vieira, J., and J. Messing.** 1987. Production of single-stranded plasmid DNA. Methods Enzymol. **153**:3–11.
60. **Weinberg, R. A., and D. R. Zusman.** 1989. Evidence that the *Myxococcus xanthus frz* genes are developmentally regulated. J. Bacteriol. **171**:6174–6186.
61. **Wylie, D., A. Stock, C.-Y. Wong, and J. Stock.** 1988. Sensory transduction in bacterial chemotaxis involves phosphotransfer between Che proteins. Biochem. Biophys. Res. Commun. **151**: 891–896.
62. **Zusman, D. R.** 1982. Frizzy mutants: a new class of aggregation-defective developmental mutants of *Myxococcus xanthus*. J. Bacteriol. **150**:1430–1437.
63. **Zusman, D. R.** 1984. Cell-cell interactions and development in *Myxococcus xanthus*. Q. Rev. Biol. **59**:119–138.